Published in final edited form as:
J Cogn Neurosci. 2012 December ; 24(12): 2334–2347. doi:10.1162/jocn_a_00307.

Columnar Processing in Primate pFC: Evidence for Executive Control Microcircuits

Ioan Opris[1], **Robert E. Hampson**[1], **Greg A. Gerhardt**[2], **Theodore W. Berger**[3], and **Sam A. Deadwyler**[1]

[1]Wake Forest School of Medicine, Winston-Salem, NC

[2]University of Kentucky

[3]University of Southern California

Abstract

A common denominator for many cognitive disorders of human brain is the disruption of neural activity within pFC, whose structural basis is primarily interlaminar (columnar) microcircuits or "mini-columns." The importance of this brain region for executive decision-making has been well documented; however, because of technological constraints, the minicolumnar basis is not well understood. Here, via implementation of a unique conformal multielectrode recording array, the role of interlaminar pFC minicolumns in the executive control of task-related target selection is demonstrated in nonhuman primates performing a visuomotor DMS task. The results reveal target-specific, interlaminar correlated firing during the decision phase of the trial between multielectrode recording array-isolated minicolumnar pairs of neurons located in parallel in layers 2/3 and layer 5 of pFC. The functional significance of individual pFC minicolumns (separated by 40 μm) was shown by reduced correlated firing between cell pairs within single minicolumns on error trials with inappropriate target selection. To further demonstrate dependence on performance, a task-disrupting drug (cocaine) was administered in the middle of the session, which also reduced interlaminar firing in minicolumns that fired appropriately in the early (nondrug) portion of the session. The results provide a direct demonstration of task-specific, real-time columnar processing in pFC indicating the role of this type of microcircuit in executive control of decision-making in primate brain.

INTRODUCTION

It has been extensively reported that most common cognitive impairments related to aging, attention-deficit hyper-activity disorder (ADHD), schizophrenia, and autism are characterized by inability to select correct behaviors for the appropriate environmental or task-related circumstances (Wang et al., 2011; Dobbs, 2010; Brennan & Arnsten, 2008; Buxhoeveden et al., 2006; Buxhoeveden & Casanova, 2002; Duncan, Johnson, Swales, & Freer, 1997; Shallice & Burgess, 1991). A common denominator of these deficits in primate brain is disruption of neural activity in pFC, which utilizes precise organization of neural firing in parallel minicolumns to coordinate attention, decision-making, and behavior (Beveridge, Gill, Hanlon, & Porrino, 2008; Weiler, Wood, Yu, Solla, & Shepherd, 2008; Rao, Williams, & Goldman-Rakic, 1999; Mountcastle, 1997). The minicolumn is a neuronal "module" (Casanova, Buxhoeveden, & Gomez, 2003; Buxhoeveden & Casanova, 2002) that integrates horizontal and vertical components of the cortical anatomy (Lund, Angelucci, &

Reprint requests should be sent to Dr. Sam A. Deadwyler, Department of Physiology and Pharmacology, Wake Forest School of Medicine, Medical Center Boulevard, Winston Salem, NC 27157, or via sdeadwyl@wakehealth.edu.

Bressloff, 2003; Tanaka, 2003; Mountcastle, 1997). It has been suggested that prefrontal cortical minicolumns form the basic units that integrate, store, and select relevant information for cognitive purposes (Opris, Hampson, Stanford, Gerhardt, & Deadwyler, 2011; Takeuchi, Hirabayashi, Tamura, & Miyashita, 2011; Casanova et al., 2008; Mountcastle, 2007). The functional role of the minicolumn emerges from pFC associational abilities to integrate sensory signals in supragranular layers (Opris et al., 2011) with behavioral information in infragranular layers (Casanova et al., 2003; Buxhoeveden & Casanova, 2002), which is conveyed to subcortical structures involved in behavioral control. Alteration of prefrontal cortical minicolumns has been documented in schizophrenic patients (Casanova et al., 2008), and it is possible that this may be a major factor in controlling successful performance involving task-specific decision-making, the principal objective of this investigation.

According to many theories of cognition, cortical mechanisms of executive decision-making coordinate and control “on-line” cognitive processes underlying behavioral selection, working memory, behavioral inhibition, and multitasking (Graybiel, 2008; Baddeley, 2002; Miller & Cohen, 2001; Miyaki et al., 2000; Goldman-Rakic, 1996; Shallice & Burgess, 1996; Posner & Snyder, 1975). Furthermore, such cognitive processing can be disrupted by extended exposure to commonly abused drugs, such as cocaine (Porter et al., 2011; Deadwyler, 2010). In particular, “behavioral selection” in humans involves attention, target/goal choice, planning and monitoring of actions, and is regarded as a facet of decision-making based on sensory evidence, expected costs and benefits associated with the outcome (Resulaj, Kiani, Wolpert, & Shadlen, 2009; Heekeren, Marrett, & Ungerleider, 2008; Pesaran, Nelson, & Andersen, 2008; Opris & Bruce, 2005; Opris, Barborica, & Ferrera, 2005a, 2005b). Decisions related to behavioral selection usually reflect the option of the highest value because only one choice can be made most of the time (Pesaran et al., 2008; Sugrue, Corrado, & Newsome, 2005), and to make the optimal selection/decision, many areas in the brain with converging inputs to the supragranular layers of the pFC are activated (Opris et al., 2011; Takeuchi et al., 2011; Kritzer & Goldman-Rakic, 1995). This raises the question as to how this area of the brain processes the information required for selection of the behavioral response directed toward a particular goal. What is presented in this study is evidence for the existence of “executive microcircuitry” within pFC, featuring subpopulations of interlaminar “cell pairs” synaptically connected via cortical minicolumns (Buffalo, Fries, Landmanc, Buschman, & Desimone, 2011; Opris et al., 2011; Takeuchi et al., 2011; Mountcastle, 1997; Kritzer & Goldman-Rakic, 1995) that coordinate the activity required to perform the behavioral selection, that is, decision-making, process. Such proposed microcircuits consist of neurons in the supragranular layers 2/3 (L2/3) that integrate sensory signals and communicate directly, via specific minicolumns, with cells in the infragranular layer 5 (L5) in prefrontal (area 46) and frontal cortical regions (Areas 6 and 8) to control target/goal “selection” as the basis for behaviorally relevant decision-making (Opris et al., 2005a, 2011; Resulaj et al., 2009; Heekeren et al., 2008; Opris, Barborica, & Ferrera, 2003). To examine this presumed executive function of pFC microcircuitry, the firing of interlaminar cell pairs located in the same prefrontal and frontal cortical minicolumns were isolated and recorded by custom designed (Opris et al., 2011) conformal multielectrode arrays (MEAs). The custom-made MEAs allowed characterization of minicolumnar features of arm controlled target selection in a cognitive task requiring working memory and image-based spatial discrimination (Heyselaar, Johnston, & Paré, 2011; Buxhoeveden et al., 2006). To test specificity of minicolumnar firing for correct performance in the task, a cognitive impairing drug, cocaine, was administered midway through the session to assess the changes in the same minicolumnar processing of performance before and after disruption in task-related accuracy.

METHODS

All animal procedures were reviewed and approved by the Institutional Animal Care and Use Committee of Wake Forest School of Medicine, in accordance with U.S. Department of Agriculture, International Association for the Assessment and Accreditation of Laboratory Animal Care, and National Institutes of Health guidelines.

Visual DMS Task

Nonhuman primates (NHPs) utilized as subjects in this study ($n = 4$) were trained for at least 2 years to perform a well characterized, custom-designed visual DMS task (Hampson, Porrino, Opris, Stanford, & Deadwyler, 2011; Opris et al., 2011) shown in Figure 1A. Animals were seated in a primate chair with a shelf-counter in front of a display screen (Figure 1A) during performance of the task. Right limb (arm) position on the counter top was tracked via a UV-fluorescent reflector affixed to the back of the wrist, which was illuminated with a 15-W UV lamp detected by a small LCD camera positioned 30 cm above the hand. Hand position and movement were digitized and displayed as a bright yellow cursor on the projection screen and horizontal positions of illuminated targets were computed from the video image using a Plexon Cineplex scanner connected to a behavioral control computer. In some cases, eye position (horizontal and vertical coordinates) was recorded at 1000 Hz resolution using the EyeLink system (EyeLink 1000, SR Research, Ontario, Canada). Trials were initiated by the animal placing the cursor inside a yellow 3-in. diameter circle (“Start” ring) randomly illuminated in one of the nine geometric spatial positions on the screen (Figure 1A), which produced a randomly chosen trial unique “Sample” clip art image displayed at one of eight screen positions for 2.0 sec (“Sample Phase”). The animal was required to place the cursor in the Sample image (Sample Response) to initiate the Delay phase in which the screen was blank for a duration of 1–60 sec, randomly selected on each trial (the focus ring was not present during the delay period). Timeout of the Delay initiated the Match phase of the task in which a screen display of two to seven trial unique clip art images, including the Sample image, were presented at separate randomly selected spatial locations at the same time. After presentation of the sample, animals were allowed to move the cursor on the target for 5.0 sec and Sample target timeouts were set at 5 sec. Placing the cursor into the Sample image during the Match phase constituted the correct “Match Response,” which produced a drop of juice delivered via a sipper tube located near the animal’s mouth and blanked the screen. The correct zone for the Match Response was limited to the target (i.e., image) dimensions and the cursor had to be placed inside the target area for at least 150–200 msec for the trial to be correct. Placement of the cursor into one of the nonmatch (distracter) images constituted a nonmatch (error) response and caused the screen to blank without reward delivery and initiated the 10-sec intertrial interval. All images (sample and distracter) were unique for each trial in sessions of 100–150 trials and were chosen from a 5000 image selection buffer which was updated with new images every month. All subjects were trained to overall performance levels of 70–75% correct on the above described DMS task parameters.

Surgery

Animals were surgically prepared with cranial access cylinders for attachment of a microelectrode manipulator over the specified brain ROIs. During surgery animals were anesthetized with ketamine (10 mg/kg), then intubated and maintained with isoflurane (1–2% in oxygen 6 l/min). Recording cylinders (Crist Instruments, Hagerstown, MD) were placed over 20-mm diameter craniotomies for electrode access (Hampson et al., 2011) to stereotaxic coordinates of the frontal cortex (25 mm anterior relative to interaural line and 12 mm lateral to midline/vertex) in the caudal region of the principal sulcus, the dorsal limb of arcuate sulcus in area 8 and the dorsal part of premotor area 6 (Figure 1C, D), areas

previously shown by PET imaging to become activated during task performance (Figure 1E; Hampson et al., 2011). Two titanium posts were secured to the skull for head restraint with titanium steel screws embedded in bone cement. Following surgery, animals were given 0.025 mg/kg buprenorphine for analgesia and penicillin to prevent infection. Recording cylinders were disinfected thrice weekly with Betadine during recovery and daily during recording. Vascular access ports (Norfolk Medical Products, Skokie, IL) for drug infusions were implanted subcutaneously in the midscapular region, the end of the catheter threaded subcutaneously to a femoral incision, inserted into the femoral vein, and threaded for a distance calculated to terminate in the vena cava. Cannulae were flushed daily with 5 ml heparinized saline needed for intravenous drug administration.

Electrophysiological Recording

Electrophysiological procedures and analysis utilized the MAP Spike Sorter by Plexon, Inc. (Dallas, TX) for 64 channel simultaneous recordings. Customized conformal designed ceramic MEAs were manufactured in collaboration with Dr. Greg Gerhardt (Center for Microelectrode Technology—CenMet, Lexington, KY) at the University of Kentucky (Hampson, Coates, Gerhardt, & Deadwyler, 2004). MEAs consisted of etched platinum pads (Figure 1E) for recording multiple single neuron activity (Hampson et al., 2011; Hampson, Pons, Stanford, & Deadwyler, 2004) from which single extracellular action potentials (Figure 2A) were isolated and analyzed with respect to firing on specific recording pads during different events within DMS trials (Figures 1–3). The model W3 configuration probe (Figure 1E) was specially designed to conform to the columnar anatomy of pFC such that the top 4 recording pads recorded activity from neurons in the supragranular L2/3 whereas the lower set of four pads simultaneously recorded neuron activity in the infragranular L5 (Figure 2A and B).

Data Analysis

Task performance was determined for each animal ($n = 4$) as percentage of correct trials within and across sessions and related to simultaneous recordings of MEA conformal multiple single neuron firings on individual trials during Match phase image selection in the task (Hampson et al., 2011). Cell types were identified as regular firing by baseline (nonevent) firing rate (Opris, Hampson, & Deadwyler, 2009) and significant changes ($z > 3.09$, $p < .001$) in firing (see below) on single trials in perievent histograms (PEHs) derived for intervals of ±2.0 sec relative to the time of Match screen presentation (0.0 sec) that signaled onset of the Match phase of the task (Figures 1–3). Task-related neural activity was classified according to locations on the conformal MEA positioned specifically in cortical L2/3 and L5 (Figure 1F) upon insertion before the start of the DMS session. To account for neuronal responses in terms of columnar microcircuit organization, pFC neurons recorded on the MEAs were characterized by (1) layer-specific firing in terms of simultaneous cell activity on both vertical sets of 1350 μm (L2/3 upper and L5 lower) isolated pads (Figure 1F) during electrode positioning and (2) whether the same cell pair firing was modulated similarly during the Match phase of the DMS task (Hampson et al., 2011). Standard scores, Z = [peak - baseline firing rate]/SD baseline firing rate, were calculated for individual cell firing on each DMS task event. Firing rate was analyzed in 250-msec bins for ±2.0 sec surrounding the time of initiation (0.0 sec) task events. Neurons were only included in the analysis if their firing rates were significantly elevated from that in the Prematch presentation (−2.0 to 0.0 sec) baseline period (Z scores, ANOVA F test $p < .01$; Figures 4D and 5D). Statistical analyses were also used to test whether there were interlaminar differences in firing rates for cells in different layers (i.e., L2/3 vs. L5) during Match phase activation. Differences in cross-correlation were assessed using standardized distributions of coefficients extracted from firing of interlaminar cell pairs under different conditions related to performance in the Match phase (Figures 2, 4, and 5). Mean CCHs were calculated and

compared relative to normalized mean coefficients for the same populations of cell pairs under different experimental conditions (Figure 2). All CCHs considered satisfied the 99% confidence limits requirement (Opris et al., 2011). The correspondence of firing between cells in different layers was tested via cross-correlation histograms (CCHs) that extracted synchronous occurrences of spikes in both layers employing L2/3 cell firing to test the synchronous discharge of simultaneously recorded L5 cells in 1.0 msec intervals over ±1.0–2.0 sec task-related events (Figure 2C). CCHs were for interlaminar cell pairs (L2/3 and L5) were generated using a “shuffle” shift predictor built into Neuro-Explorer (www.neuroexplorer.com/), which computed random cross-correlation levels because of chance by randomizing the actual spike sequence and calculating the cross-correlation five different times for a given pair of neurons. The “shift-predicted” chance correlation factor was then subtracted from the true coefficients for CCHs to adjust for differences in cell firing rates and frequency of bursting (Opris et al., 2011; Takeuchi et al., 2011). Population (mean) CCHs were computed by averaging coefficients across multiple cell pairs and plotting the mean values (±*SEM*) in 1.0 msec bins (Figures 4E and 5E).

Tuning Plots

For each interlaminar cell pair (L2/3 and L5) firing on the same trials was plotted with respect to the position of the match target selected and responded to as a response in the Match phase (Figure 3). Directionality was assigned according to the eight positions on the screen with reference to placement of the cursor in the center providing angular directions corresponding to the location of the match image around the periphery of the screen, yielding 0° (directly lateral), 45°, 90°, 135°, 180°, 225°, 270°, 315°, and 360° movement directions from center of screen (Felsen et al., 2002; Rao et al., 1999). Mean firing rate commencing at Match phase onset until time of occurrence of the Match Response (i.e., typically 0.5–1.0 sec; Figures 4D and 5D) was calculated for the position of the response on each trial and represented in polar coordinates as tuning plots of the average firing rate for each interlaminar cell pair over all trials in a single session. A directional bias or “preference” for a given cell pair was revealed by response locations with the highest mean firing rates with respect to all the other positions responded to during the session (Figure 3B). Average tuning plots (Figure 3C) were constructed by averaging firing rates of cells in each layer for each screen position over all trials across all sessions.

Drug Administration

Animals were trained to perform the task with intravenous saline injections into the vascular access port or saphenous vein of the left leg before and midway through DMS testing sessions. On days in which cocaine was administered, midsession saline injections were replaced with intravenous injection of cocaine (0.4 mg/kg), via the same route (Hampson et al., 2011).

Identification of Cortical Layers and Minicolumns

The conformal MEA (model W3) probe (Figure 1E) was specially designed such that the two sets of recording pads could only record simultaneous activity from neurons separated by 1300 μm, which given its orientation of insertion into pFC (dorsal premotor gyrus in area 6, stereotactic coordinates AP:25 and ML:12) constituted firing of cells in infragranular L5 and supragranular L2/3 (Hansen & Dragoi, 2011; Opris et al., 2011; Takeuchi et al., 2011; Hampson, Coates, et al., 2004) as shown in Figure 1F. Misplacement of the probe due to different angular penetration relative to columnar orientation in pFC was blatantly signaled by the absence of simultaneous cell recordings on both of the sets of pads separated vertically by 1300 μm. The MEA (Opris et al., 2011; Hampson, Coates, et al., 2004) employed here allowed to recording of pFC columnar activity in two dimensions rather than one (Hansen & Dragoi, 2011; Mo, Schroeder, & Ding, 2011; Takeuchi et al., 2011) because,

with proper vertical alignment (<5.0°), activity from two different adjacent minicolumns could be detected and validated as shown in (Figure 2).

RESULTS

Four rhesus (*Macaca mulatta*) NHPs were trained to perform a DMS task (Hampson et al., 2011; Deadwyler, Porrino, Siegel, & Hampson, 2007; Porrino, Daunais, Rogers, Hampson, & Deadwyler, 2005), which required selecting the same video image presented on-screen in the prior Sample phase from a set of two to seven images in the subsequent Match phase after an intervening Delay of 1–60 sec (Figure 1A). The NHPs made hand tracking movements of a cursor on the screen in the Match phase to obtain a juice reward for selection of the correct (Sample) image in different positions which varied on each trial with respect to image type and screen position. Key variables in the task were (a) number of images (2–7) presented in the Match phase, (b) duration of the delay (1–60 sec), and (c) the random placement of the Sample (target) image in one of seven spatial positions on the screen in the Match phase (after the delay interval) that differed from the position in the Sample phase. Previous work with the same DMS task has validated necessity of attention, STM and response latency, together with influences of choice factors, cognitive workload, and reward expectancy (Deadwyler et al., 2007; Porrino et al., 2005); however, recent analyses indicated that animals were executing a “decision process” in the Match phase of the task (Figure 1A) involving target selection which is described here in relation to neuron firing in pFC (Hampson et al., 2011). The total number of cells recorded in this study was 378 from four NHPs (62 cells in animal “K,” 46 cells in animal “B,” 38 in animal “E,” and 34 in animal “G”), 195 of cells were recorded from L2/3, and 183 cells from L5. These cells were the basis for the selection of interlaminar pairs, 90/195 cells (46%) from L2/3, and 90/183 (49%) from L5. Overall these 180 putative pyramidal cells yielded 90 interlaminar pairs with regular spiking (60 pairs in the correct vs. error analysis and 30 pairs in the cocaine study described below). Fast spiking inter-neurons and cells with inhibitory or no response to the designated task events were not included in this analysis.

MEA Recordings from Cortical Layers and Minicolumns

Prior reports of neural correlation with executive function and decision-making in a sensorimotor hierarchy (Heekeren et al., 2008; Pesaran et al., 2008; Opris & Bruce, 2005; Miller & Cohen, 2001) refer to recordings made in dorsolateral pFC as shown in Figure 1B and C, which were also reported to depend on the interaction between neurons in different layers in that same cortical area (Opris et al., 2011; Takeuchi et al., 2011; Goldman-Rakic, 1996). In this study interlaminar connectivity was sensed by conformal-designed MEAs (Figure 1D and E) positioned to simultaneously record neurons located in pFC L2/3 and L5 in adjacent “minicolumns” during performance of the DMS task as shown in Figure 1F. A key factor in the identification of cortical layers and minicolumns relates to the configuration of the W3 MEA employed as shown in Figure 1E. The MEA contained two linear sets of four recording pads separated vertically by 1350 μm to conform to the distance between pFC cortical cell L2/3 and L5 when positioned perpendicular to the parallel lamellae (see Methods section). The two sets of dual vertically placed pads in each upper and lower position on the MEA were separated horizontally by 40 μm to exceed the reported 28 μm width of single cortical mini-columns (Opris et al., 2011; Casanova, Trippe, Tillquist, & Switala, 2009). This allowed recording from two adjacent L2/3 and L5 cell pairs constituting activity from two separate minicolumns on a single MEA probe. This pad configuration insured that only cells in L2/3 and L5 were recorded, because the appearance of cells simultaneously on both vertically arranged sets of pads required 0° angular placement relative to both cell layers (Takeuchi et al., 2011) as shown in Figure 1D. In this study spatiotemporal analyses of 180 prefrontal cortical pyramidal cells recorded in four

NHPs revealed a large number ($n = 60$) of L2/3 and L5 cell pairs in pFC that displayed interlaminar interactions during the Match phase of the DMS task.

Columnar Processing in pFC during "Target Selection" Phase of DMS Task

The relevance of minicolumnar activity to decision-making has been investigated under several conditions (Opris et al., 2011; Resulaj et al., 2009; Heekeren et al., 2008; Pesaran et al., 2008; Opris & Bruce, 2005; Goldman-Rakic, 1996). An example of this interlaminar interaction during the target selection, Match phase of the task (Figure 1A), is shown in Figure 2A and B for two cell pairs with raster/PEHs bracketing the temporal interval of image presentation (Match phase onset) and completion of the target selection Match Response ($M = 0.0 \pm 2.0$ sec). The cell pairs were recorded on appropriate sets of adjacent pads (Minicolumns 1 and 2) in the conformal MEA shown in the illustration of both interlaminar cell pairs in L2/3 and L5 (Figure 2A and B). Neurons in both layers showed significant increases in mean firing (L2/3: $F(1, 158) = 20.83$, $p < .001$; L5: $F(1, 158) = 22.56$, $p < .001$) as a function of Match screen presentation (Postmatch: $M = 0.0$ to $+2.0$ sec) and during subsequent movements associated with target selection (Figure 1A) characteristic of decision-making in this task (Hampson et al., 2011), relative to the same time period before Match phase onset (Prematch: −2.0 to 0.0 sec). A consistent finding employing this recording configuration was the observation within neuron pairs in the same minicolumn, L2/3 cells consistently exhibited significantly higher mean firing rates in the 0.0 + 2.0 sec interval after Match phase onset (Figure 2, upper raster/PEHs) than neurons in L5 (lower raster/PEHs) over the same temporal interval, $F(1, 158) = 15.73$, $p < .001$. Demonstration of more precise functional connections between individual cells within each minicolumn was provided by CCHs (Hong, Ratté, Prescott, & De Schutter, 2012; Opris et al., 2011; Takeuchi et al., 2011) constructed for individual L2/3 and L5 cell pairs recorded on vertically positioned pads of the MEA (Figure 1F). Normalized CCHs for both minicolumn cell pairs are shown in Figure 2A and B for cell firing in the displayed PEHs (i) before (black curve) Match phase onset (−2.0 to 0.0 sec, Pre) or (ii) after (green) Match phase onset (0 to +2.0 sec, Post) for the same cell pairs. Although both CCHs show significantly correlated firing (Pre: $Z = 13.27$, $p < .001$; Post: $Z = 11.16$, $p < .001$), the differences in peak correlation for both cell pairs indicate that interlaminar firing was more synchronized after Match image presentation and during movements for target selection (0.0–2.0 sec) than in the prior baseline (−2.0 to 0.0 sec) period (pair wise comparison; Pre vs. Post $F(1, 401) = 11.46$, $p < .001$). Finally, the most important demonstration of the MEA specificity for detecting true columnar activity was demonstrated by the lack of significant ($Z = 1.66$, $p > .05$) correlations between the firing of L2/3 cells in Minicolumn 1 and L5 cells in the adjacent Minicolumn 2 on the same MEA probe, when assessed in the same task phase as shown in Figure 2C (diagonal CCH).

Another way of analyzing minicolumnar processing was provided by examining "tuning plots" (Felsen et al., 2002; Rao et al., 1999) of pFC cell pairs that were constructed for each of the target positions on the screen where placement of the cursor in the Match phase of the task was required on different trials in the session (Figure 1A). Columnar recording by the MEA could be verified if the alignment of firing biases in both cortical layers (i.e., cell pairs) were the same selected target locations on the screen (Opris et al., 2011; Zhang & Alloway, 2006; Felsen et al., 2002) during the Match phase. It has been demonstrated that such decision-making relies on networks of pyramidal neurons that interconnect with each other in laminar–columnar neuronal arrays (Opris et al., 2011; Pesaran et al., 2008; Sugrue et al., 2005). Neurons in L2/3 and L5 fire more to the same preferred spatial location in cortical minicolumns (Rao et al., 1999); however, when movement choices vary from trial-to-trial as in this task (Figure 1A) neurons in L2/3 and L5 must coordinate their activity (Opris et al., 2011; Pesaran et al., 2008) and that is shown here (Figure 3) to be controlled by

columnar processing. Figure 3A shows an example of L2/3 cell firing onset during Match phase screen presentation (Figure 2) accompanied by the saccadic eye movements reflecting visual search for the Match image. Figure 3B shows PEHs of average firing rates for both L2/3 (blue) and L5 (red) cells recorded in the same MEA minicolumn (Figure 2) that exhibited similar alterations in firing over the eight different locations on the screen for target presentation (Figure 1A), summed over all trials in a single session. This type of mini-columnar correspondence was also reflected by "tuning biases" or higher firing rates in one versus other screen locations, which were the same for both cells in the mini-columnar pair (Figure 3B, lower left; 180° asterisk). This was even more supportive of selective minicolumnar processing by the fact that for different minicolumns tuning biases differed, which is illustrated in Figure 3C by the display of tuning plots from six different minicolumnar cell pairs (L2/3 upper and L5 lower). Differences in overall mean firing rate during target selection at biased versus nonbiased locations is shown in Figure 3D summed over multiple cell pairs ($n = 14$) in which firing in one (biased) location was higher than the average rate in the other seven locations for both the L2/3 and L5 cells, $F(1, 167) = 11.78$, $p < .001$. Moreover, comparison of mean inter-laminar CCHs (Figure 2A and B) with respect to synchronized firing at preferred (biased) versus nonpreferred target locations was also significantly higher between the same minicolumnar cell pairs shown in Figure 3D, $F(1, 167) = 8.52$, $p < .01$.

To test whether the increase in correlated firing between L2/3 and L5 cell pairs was specific to task-related image selection in the Match phase, similar analyses were performed on correct versus error trials within the same session. Figure 4A shows that the same minicolumnar cell pair that exhibited increased firing during the Match phase on correct trials (left) showed reduced firing on trials in which the inappropriate image was selected on error trials (right). Figure 4B shows that this was associated with a significant decrease in correlated firing between the same cell pair on error vs. correct trials, $F(1, 401) = 18.64$, $p < .001$, and was shown not to be due to alterations in firing rate per se (Hong et al., 2012). The relevance of this change in inter-laminar peak correlation to a direct influence on cognitive performance (Robbins & Arnsten, 2009) was revealed by the altered shape of the tuning plot (Felsen et al., 2002; Rao et al., 1999) for the same cell pair (Figure 4C) on error trials in which both cells exhibited reduced rates of firing at each target-screen location. Also, the L5 cell showed a loss firing bias (Figure 4C, 135° position) on error versus correct trials on trials, but this change in location bias did not occur in the L2/3 neuron firing even though the firing rate was reduced as occurred at all screen locations. These same changes with respect to correct versus error trials were present across all pFC L2/3 and L5 cell pairs evaluated ($n = 60$) as shown in Figure 4D for the mean ($\pm SEM$) firing rate change on correct (blue) and error (red) trials within the same DMS sessions averaged over the same Match phase interval as shown in Figure 4A. Mean firing rates (0.0 to +2.0 sec) were significantly higher for L2/3 versus L5 cells under both conditions, $F(1, 958) = 6.27$, $p < .01$, but rates for both L2/3 and L5 cells were significantly lower on error versus correct trials [L2/3: $F(1, 958) = 11.12$, $p < .001$, L5: $F(1, 958) = 6.67$, $p < .01$, $n = 60$; ANOVA]. As confirmation of the lack of interlaminar correlated firing between L2/3 and L5 on error trials (Figure 4B), Figure 4E shows a significant reduction in the mean CCH peak correlations, $F(1, 119) = 14.18$, $p < .001$ (and for inset CCHs, $F(1, 598) = 11.34$, $^{**}p < .001$; ANOVA), constructed from the same cell pairs ($n = 60$) shown in Figure 4D. The distributions of latencies for the Match Response are displayed as histograms in Figure 4D, which show no differentiation with respect to time of target selection for correct (blue) versus error (red) trials, thereby eliminating arm movement as a possible basis for the differences in minicolumnar processing.

Cocaine Administration Modifies Dopamine Influence on pFC Columnar Processing

Extensive prior investigation of features that affect cognitive processing in DMS tasks have shown that Match phase activation of pFC is altered by many factors (Hampson et al., 2011) including modulation of dopamine influences on task-related pFC cell firing (Robbins & Arnsten, 2009). Consistent with this notion, pFC neural firing was investigated recently after systemic injections of cocaine in animals performing this DMS task and showed decreased activity across all trials, which increased the chance of error and reduced performance accuracy (Hampson et al., 2011). However, in that study the specific influence of the drug on columnar processing was not determined, therefore interlaminar (L2/3 and L5) cell pairs in pFC ($n = 30$) were recorded in the same manner as shown in Figures 1–4 but with cocaine administered unsignaled via acute intravenous injection (0.4 mg/kg) midway through the session. This was done so that the effects of the drug could be assessed on the same interlaminar cell pairs pre-recorded in the first half of the session under normal (saline iv administration) conditions. Figure 5A shows firing in raster/PEHs for a pFC interlaminar cell pair (L2/3 upper, L5 lower), (1) recorded in the first 60 trials of the DMS session (Control) followed by (2) activity assessed in the second half of the same session (120 total trials) in which cocaine was administered (iv) at Trial 61 (Figure 5A, cocaine). Administration of cocaine produced a reduction in Match phase firing of L2/3 cell, $F(1, 158) = 19.72$, $p < .001$, but not L5 cell, $F(1, 158) = 1.14$, $p > .05$, *ns*, in the second half of the session compared with firing of the same cell pair in the saline control half of the session (Figure 5A). In addition, a significant reduction in peak correlation between the same cell pair, $F(1, 401) = 17.22$, $p < .001$, was exhibited in the cocaine versus control (saline) half of the session (Figure 5B). These reductions in interlaminar cell firing and correlation from preadministration levels resembled closely those shown for error vs. correct trials in Figure 4A and B. These changes were also accompanied by alterations in the spatial tuning plot (Figure 4C) for the same cell pair (Figure 5A) in the cocaine half of the session compared with the saline control (Figure 5C) half of the session, $F(1, 79) = 11.69$, $p < .001$. Firing at all locations was reduced in both cells following cocaine administration, but the same spatial bias location was maintained in the tuning plots of both cells (Figure 5C, 0°). Finally, the generality of the suppressive effect of cocaine on Match phase mean firing rate over all cell pairs ($n = 30$) is shown in Figure 5D as a significant decrease in L2/3 cell activity, $F(1, 958) = 13.43$, $p < .001$, relative to the saline half of the session. L5 average firing rate was not significantly reduced, $F(1, 958) = 1.48$, $p > .05$, *ns*. More importantly, Figure 5E indicates that there was a marked reduction in L2/3 and L5 firing synchrony after cocaine administration, as a significant reduction, $F(1, 59) = 11.22$, $p < .001$, in the mean CCH peak correlation of intercolumnar activity averaged over the same cell pairs ($n = 30$) shown in Figure 5D. The inset in Figure 5E shows that the reduction in average peak CCHs on cocaine trials was also associated with reduced firing synchrony on correct trials in the cocaine half of the session compared with initial, normal firing, on correct trials.

Effects of Cocaine-altered pFC Columnar Processing on DMS Performance

Consistent with previous reports in this laboratory, cognitive workload (number of images in the Match phase and duration of delay) in the DMS task was manipulated by increasing visual complexity and/or duration of delay on each trial (Hampson et al., 2011; Deadwyler, 2010). PET imaging of [^{18}F]fluorodeoxyglucose uptake in brains of NHPs performing the same DMS task has demonstrated differential processing by separate brain areas depending on cognitive workload (Robbins & Arnsten, 2009; Deadwyler et al., 2007; Porrino et al., 2005). Both neuronal and metabolic activity in these same prefrontal areas has been shown to be altered by cocaine, which impaired performance on high cognitive workload trials (Hampson et al., 2011). Figure 6A shows results consistent with these prior findings and tracks the change in performance in the same session shown in Figure 5A–C on a trial-by-trial basis with injection midway through the session. It is clear that as the number of trials

progressed the even distribution of error versus correct trials in the first half of the session (Control) changed after cocaine administration (Trial 61) to more cumulative errors relative to fewer correct trials in the second half of the same session. Figure 6B shows the effects of cocaine on task performance in the second half of the session with respect to cognitive load (Hampson et al., 2011) indicated by the decrease, $F(1, 96) = 12.33$, $p < .001$, in the mean percent correct responses as a function of the increase in the number of distracters (Images 2–7) in the Match phase during target selection. In association with this decrement in DMS performance midsession injection of cocaine produce a significant decrease in inter-laminar cross-correlations (Figure 5E) compared with correlations of the same cell pairs ($n = 30$) in the Control half of the session. The scatter plot of normalized cross-correlation coefficients in Figure 6C shows that those cell pairs with lower correlation coefficients in the Control half of the session exhibited less change (diagonal line) following cocaine injection than cell pairs with higher coefficients (≥0.04) in the Control half of the session, $F(1, 59) = 11.22$, $p < .001$. Thus, the higher the interlaminar correlation under normal conditions, the more likely cocaine reduced that correlation in the same cell pair in the second half of the DMS session. This is illustrated in Figure 6D as a cocaine-induced decreased columnar transmission between L2/3 and L5 cells, which under normal (nondrug) conditions exhibited high levels of firing synchrony as shown in Figure 6C.

DISCUSSION

Response-Dependent Columnar Processing in pFC

The findings reported here (Figures 2, 3, and 4) are consistent with the idea that neurons in the supra- and infragranular layers form efficient minicolumnar circuits during the Match phase target selection process required for effective performance of tasks such as this one (Buffalo et al., 2011; Opris et al., 2011; Takeuchi et al., 2011; Resulaj et al., 2009; Pesaran et al., 2008; Swadlow, Gusev, & Bezdudnaya, 2002). The unique conformal ceramic (MEA) recording probe (Figure 1E) employed in this study provided the basis for this first time assessment of interlaminar correlated firing (Opris et al., 2011) validated in multiple recordings of L2/3 and L5 cell pairs that yielded similar relations following several manipulations and treatments across animals and sessions (Figures 3D, 4E, and 5E). The increase in L2/3 and L5 correlation specific to the decision for target selection in the Match phase of the task (Figures 2, 4, and 5) suggests that a key variable in DMS task-related performance was activation of L5 neurons via specific minicolumnar input from paired neurons in L2/3, which have been shown to participate in the integration of sensory evidence with “long-range” inputs from the dorsal visual stream, in parietal/visual cortex (Resulaj et al., 2009; Heekeren et al., 2008; Pesaran et al., 2008; Opris & Bruce, 2005). Such integration was definitely reduced on error trials as indicated by the reduction in firing synchrony between L2/3 and L5 cell pairs relative to correct trials under normal performance conditions (Figure 4B and E). Another feature demonstrating the columnar nature of this type of multineuron processing was the fact that classified cell pairs also showed the same Match phase spatial tuning biases (Felsen et al., 2002) during the session (Figure 3), which indicates the presence of previously identified pFC minicolumnar selection biases (Opris et al., 2011; Resulaj et al., 2009; Rao et al., 1999).

pFC minicolumn has been regarded as a neuronal “module” (Casanova et al., 2003; Buxhoeveden & Casanova, 2002) with basic associative abilities to integrate the horizontal (or bottom–up sensory processing) and vertical (top–down) “components” of cortical integration (Mountcastle, 2007; Lund et al., 2003; Tanaka, 2003). Thus, neurons in supragranular layers have been shown to extend “long-range” feed-forward/feedback connections between primary sensory areas and pFC prividing input to minicolumns in L2/3 (Kritzer & Goldman-Rakic, 1995), whereas neurons in the infragranular layers that participate in the inter-laminar minicolumnar processing in L/5 provide the output to the

subcortical structures involved in behavioral responding (Wagatsuma, Potjans, Diesmann, & Fukai, 2011). Alteration/disruption of prefrontal cortical minicolumns has been documented in schizophrenic and autistic patients that show cognitive deficits (Casanova et al., 2003, 2008; Buxhoeveden & Casanova, 2002).

Pharmacological Disruption of Task-related Cortical Columnar Processing

As described above, reduced correlation of firing between the same interlaminar cell pairs (n = 60) in the Match phase of the task distinguished correct versus error trials (Figure 4B and E) across all animals. A similar reduction in correlated firing was also shown for minicolumn cell pairs following cocaine administration midway through the session (Figure 5B and D). This drug-induced reduction in synchronized firing, even on correct trials (Figure 5E), could have produced increased susceptibility to incorrect choices on the more difficult (increased number of images) trials in the DMS task (Figure 6B and C). In addition, cocaine administration reduced firing to all locations in a manner similar to that on error trials (Figure 5C) but interestingly did not alter the tuning biases of the same cell pairs. Figure 6C shows that the loss in correlation produced by cocaine was most extreme for pairs of cells that exhibited high correlation values in the control (saline) first half of the session whereas cell pairs with low normalized correlations (<0.04) were relatively unaffected by cocaine administration in the second half of the session. These findings are in close agreement with prior studies showing marked influences of acute administered cocaine in altering task-related neural firing (Hampson et al., 2011; Opris et al., 2009; Anderson et al., 2008; Rebec & Sun, 2005; Stuber, Roitman, Phillips, Carelli, & Wightman, 2005; Volkow et al., 2005; Bradberry, 2000) and support the notion that dopaminergic modulation of pFC neuron firing may be responsible for regulating columnar processing in a manner that controls decision-making and target selection in cognitive tasks (Seong & Carter, 2012; Porter et al., 2011; Graybiel, 2008; Opris et al., 2005a, 2005b; Volkow et al., 2005; Rao et al., 1999).

Conclusion

These unique results show that columnar interactions between pFC neurons that encode and process information relevant to executive function and decision-making (Opris & Bruce, 2005; Miller & Cohen, 2001; Goldman-Rakic, 1996) are necessary for successful performance of the DMS task (Figures 2–4) which can be disrupted by acute administration of cocaine (Figures 5 and 6). The possible neural basis for effective performance in this task therefore relates to the significantly increased transmission within pFC minicolumns that provides a “selection bias” (Figure 3B) from similar interlaminar correlated L2/3 and L5 cell pairs during the decision phase of the DMS task (Figures 4E and 5E). Also, as demonstrated here, task performance as well as interlaminar cell firing were both disrupted by cocaine administration during the same session (Figure 5), thereby indicating that columnar specific synchronous firing between L2/3 and L5 cell pairs was the critical factor for successful performance of the task (Porter et al., 2011). Previously reported actions of cocaine on dopamine receptor-mediated processes that could have provoked a disruption in minicolumnar firing include (1) cocaine altered correlates of task-activation in pFC (Rebec & Sun, 2005; Stuber et al., 2005; Volkow et al., 2005; Felsen et al., 2002; Bradberry, 2000) and/or (2) the well-known cocaine modulation of dopamine release and reuptake in pFC cells (Shohamy & Adcock, 2010; Anderson et al., 2008; Nestler, 2004). These findings (Figures 5 and 6) also provide additional evidence for abuse-related cognitive disruption in humans following excessive drug abuse (Lucantonio, Stalnaker, Shaham, Niv, & Schoenbaum, 2012; Tomasi et al., 2010). However because the average firing rate of L5 neurons was not affected significantly by cocaine administration (Figure 5D), cocaine actions in this study were mediated by reduction in the firing of L2/3 cells, which reduced columnar input to L5 cells. Finally, this demonstration of performance-related minicolumnar

processing could provide insight into the basis for other types of cognitive impairments involving decision-making and executive function in humans as a result of disease, injuries, or other disorders (Wang et al., 2011; Dobbs, 2010; Brennan & Arnsten, 2008; Buxhoeveden et al., 2006; Duncan et al., 1997; Shallice & Burgess, 1991).

Acknowledgments

We thank Joshua Long, Joseph Noto, Brian Parish, Joshua Fuqua, Mack Miller, and Shahina Kozhisseri for their assistance on this project. This work was supported by National Institutes of Health grants DA06634, DA023573, DA026487, and by Defense Advanced Research Projects Agency (DARPA) contract N66601-09-C-2080 to S. A. D. and by NSF grant EEC-0310723 and DARPA contract N66601-09-C-2081 to T. W. B.

References

Anderson SM, Famous KR, Sadri-Vakili G, Kumaresan V, Schmidt HD, Bass CE, et al. CaMKII: A biochemical bridge linking accumbens dopamine and glutamate systems in cocaine seeking. Nature Neuroscience. 2008; 11:344–353.

Baddeley, A. Fractionating the central executive. In: Stuss, DT.; Knight, RT., editors. Principles of frontal lobe function. New York: Oxford University Press; 2002. p. 246-260.

Beveridge TJ, Gill KE, Hanlon CA, Porrino LJ. Review. Parallel studies of cocaine-related neural and cognitive impairment in humans and monkeys. Philosophical Transactions of the Royal Society of London, Series B, Biological Sciences. 2008; 363:3257–3266.

Bradberry CW. Acute and chronic dopamine dynamics in a nonhuman primate model of recreational cocaine use. Journal of Neuroscience. 2000; 20:7109–7115. [PubMed: 10995858]

Brennan AR, Arnsten AF. Neuronal mechanisms underlying attention deficit hyperactivity disorder: The influence of arousal on prefrontal cortical function. Annals of the New York Academy of Sciences. 2008; 1129:236–245. [PubMed: 18591484]

Buffalo EA, Fries P, Landmanc R, Buschman TJ, Desimone R. Laminar differences in gamma and alpha coherence in the ventral stream. Proceedings of the National Academy of Sciences, USA. 2011; 108:11262–11267.

Buxhoeveden DP, Casanova MF. The minicolumn hypothesis in neuroscience. Brain. 2002; 125:935–951. [PubMed: 11960884]

Buxhoeveden DP, Semendeferi K, Buckwalter J, Schenker N, Switzer R, Courchesne E. Reduced minicolumns in the frontal cortex of patients with autism. Neuropathology and Applied Neurobiology. 2006; 32:483–491. [PubMed: 16972882]

Casanova MF, Buxhoeveden D, Gomez J. Disruption in the inhibitory architecture of the cell minicolumn: Implications for autism. Neuroscientist. 2003; 9:496–507. [PubMed: 14678582]

Casanova MF, Kreczmanski P, Trippe J II, Switala A, Heinsen H, Steinbusch HW, et al. Neuronal distribution in the neocortex of schizophrenic patients. Psychiatry Research. 2008; 158:267–277. [PubMed: 18280583]

Casanova MF, Trippe J II, Tillquist C, Switala AE. Morphometric variability of minicolumns in the striate cortex of Homo sapiens, Macaca mulatta, and Pan troglodytes. Journal of Anatomy. 2009; 214:226–234. [PubMed: 19207984]

Deadwyler SA. Electrophysiological correlates of abused drugs: Relation to natural rewards. Annals of the New York Academy of Sciences. 2010; 1187:140–147. [PubMed: 20201851]

Deadwyler SA, Porrino L, Siegel JM, Hampson RE. Systemic and nasal delivery of orexin-A (Hypocretin-1) reduces the effects of sleep deprivation on cognitive performance in nonhuman primates. Journal of Neuroscience. 2007; 27:14239–14247. [PubMed: 18160631]

Dobbs D. Schizophrenia: The making of a troubled mind. Nature. 2010; 468:154–156. [PubMed: 21068803]

Duncan J, Johnson R, Swales M, Freer C. Frontal lobe deficits after head injury: Unity and diversity of function. Cognitive Neuropsychology. 1997; 14:713–741.

Felsen G, Shen YS, Yao H, Spor G, Li C, Dan Y. Dynamic modification of cortical orientation tuning mediated by recurrent connections. Neuron. 2002; 36:945–954. [PubMed: 12467597]

Goldman-Rakic PS. The prefrontal landscape: Implications of functional architecture for understanding human mentation and the central executive. Philosophical Transactions of the Royal Society of London, Series B, Biological Sciences. 1996; 351:1445–1453.

Graybiel AM. Habits, rituals, and the evaluative brain. Annual Review of Neuroscience. 2008; 31:359–387.

Hampson RE, Coates TD Jr, Gerhardt GA, Deadwyler SA. Ceramic-based micro-electrode neuronal recordings in the rat and monkey. Proceedings of the Annual International Conference of the IEEE Engineering in Medicine and Biology Society (EMBS). 2004; 25:3700–3703.

Hampson RE, Pons TP, Stanford TR, Deadwyler SA. Categorization in the monkey hippocampus: A possible mechanism for encoding information into memory. Proceedings of the National Academy of Sciences, USA. 2004; 101:3184–3189.

Hampson RE, Porrino LJ, Opris I, Stanford T, Deadwyler SA. Effects of cocaine rewards on neural representations of cognitive demand in nonhuman primates. Psychopharmacology (Berlin). 2011; 213:105–118. [PubMed: 20865250]

Hansen B, Dragoi V. Adaptation-induced synchronization in laminar cortical circuits. Proceedings of the National Academy of Sciences, USA. 2011; 108:10720–10725.

Heekeren HR, Marrett S, Ungerleider LG. The neural systems that mediate human perceptual decision-making. Nature Reviews Neuroscience. 2008; 9:467–479.

Heyselaar E, Johnston K, Paré M. A change detection approach to study visual working memory of the macaque monkey. Journal of Vision. 2011; 11:1–10.

Hong S, Ratté S, Prescott SA, De Schutter E. Single neuron firing properties impact correlation-based population coding. Journal of Neuroscience. 2012; 32:1413–1428. [PubMed: 22279226]

Kritzer MF, Goldman-Rakic PS. Intrinsic circuit organization of the major layers and sublayers of the dorsolateral prefrontal cortex in the rhesus monkey. Journal of Comparative Neurology. 1995; 359:131–143. [PubMed: 8557842]

Lucantonio F, Stalnaker TA, Shaham Y, Niv Y, Schoenbaum G. The impact of orbitofrontal dysfunction on cocaine addiction. Nature Neuroscience. 2012; 15:358–366.

Lund JS, Angelucci A, Bressloff PC. Anatomical substrates for functional columns in macaque monkey primary visual cortex. Cerebral Cortex. 2003; 13:15–24. [PubMed: 12466211]

Miller EK, Cohen JD. An integrative theory of prefrontal cortex function. Annual Review of Neuroscience. 2001; 24:167–202.

Miyaki A, Friedman N, Emerson M, Witzki A, Howerter A, Wagner T. The unity and diversity of executive functions and their contributions to complex frontal lobe tasks: A latenet variable analysis. Cognitive Psychology. 2000; 41:49–100. [PubMed: 10945922]

Mo J, Schroeder CE, Ding M. Attentional modulation of alpha oscillations in macaque inferotemporal cortex. Journal of Neuroscience. 2011; 31:878–882. [PubMed: 21248111]

Mountcastle VB. The columnar organization of the neocortex. Brain. 1997; 120:701–722. [PubMed: 9153131]

Nestler EJ. Historical review: Molecular and cellular mechanisms of opiate and cocaine addiction. Trends in Pharmacological Sciences. 2004; 25:210–218. [PubMed: 15063085]

Opris I, Barborica A, Ferrera VP. Comparison of performance on memory-guided saccade and delayed spatial match-to-sample tasks in monkeys. Vision Research. 2003; 43:321–332. [PubMed: 12535990]

Opris I, Barborica A, Ferrera VP. Microstimulation of dorsolateral prefrontal cortex biases saccade target selection. Journal of Cognitive Neuroscience. 2005a; 17:893–904. [PubMed: 15969908]

Opris I, Barborica A, Ferrera VP. Effects of electrical microstimulation in monkey frontal eye field on saccades to remembered targets. Vision Research. 2005b; 45:3414–3429. [PubMed: 15893784]

Opris I, Bruce CJ. Neural circuitry of judgment and decision mechanisms. Brain Research Reviews. 2005; 48:509–526. [PubMed: 15914255]

Opris I, Hampson RE, Deadwyler SA. The encoding of cocaine vs. natural rewards in the striatum of nonhuman primates: Categories with different activations. Neuroscience. 2009; 163:195–204.

Opris I, Hampson RE, Stanford TR, Gerhardt GA, Deadwyler SA. Neural activity in frontal cortical cell layers: Evidence for columnar sensorimotor processing. Journal of Cognitive Neuroscience. 2011; 23:1507–1521. [PubMed: 20695762]

Pesaran B, Nelson MJ, Andersen RA. Free choice activates a decision circuit between frontal and parietal cortex. Nature. 2008; 453:406–409. [PubMed: 18418380]

Porrino LJ, Daunais JB, Rogers GA, Hampson RE, Deadwyler SA. Facilitation of task performance and removal of the effects of sleep deprivation by an ampakine (CX717) in nonhuman primates. PLoS Biology. 2005; 3:e299. [PubMed: 16104830]

Porter JN, Olsen AS, Gurnsey K, Dugan BP, Jedema HP, Bradberry CW. Chronic cocaine self-administration in rhesus monkeys: Impact on associative learning, cognitive control, and working memory. Journal of Neuroscience. 2011; 31:4926–4934. [PubMed: 21451031]

Posner, M.; Snyder, C. Attention and cognitive control. In: Solso, R., editor. Information processing and cognition: The Loyola Symposium. Hillsdale, NJ: Erlbaum; 1975. p. 55-82.

Rao SG, Williams GV, Goldman-Rakic PS. Isodirectional tuning of adjacent interneurons and pyramidal cells during working memory: Evidence for microcolumnar organization in pFC. Journal of Neurophysiology. 1999; 81:1903–1916. [PubMed: 10200225]

Rebec GV, Sun W. Neuronal substrates of relapse to cocaine-seeking behavior: Role of prefrontal cortex. Journal of the Experimental Analysis of Behavior. 2005; 84:653–666. [PubMed: 16596984]

Resulaj A, Kiani R, Wolpert DM, Shadlen MN. Changes of mind in decision-making. Nature. 2009; 461:263–266. [PubMed: 19693010]

Robbins TW, Arnsten AF. The neuropsychopharmacology of fronto-executive function: Monoaminergic modulation. Annual Review of Neuroscience. 2009; 32:267–287.

Seong HJ, Carter AG. D1 receptor modulation of action potential firing in a subpopulation of layer 5 pyramidal neurons in the prefrontal cortex. Journal of Neuroscience. 2012; 32:10516–10521. [PubMed: 22855801]

Shallice T, Burgess PW. Deficits in strategy application following frontal lobe damage in man. Brain. 1991; 114:727–741. [PubMed: 2043945]

Shallice T, Burgess P. The domain of supervisory processes and temporal organization of behaviour. Philosophical Transactions of the Royal Society of London, Series B, Biological Sciences. 1996; 351:1405–1411.

Shohamy D, Adcock RA. Dopamine and adaptive memory. Trends in Cognitive Sciences. 2010; 14:464–472. [PubMed: 20829095]

Stuber GD, Roitman MF, Phillips PE, Carelli RM, Wightman RM. Rapid dopamine signaling in the nucleus accumbens during contingent and noncontingent cocaine administration. Neuropsychopharmacology. 2005; 30:853–863. [PubMed: 15549053]

Sugrue LP, Corrado GS, Newsome WT. Choosing the greater of two goods: Neural currencies for valuation and decision making. Nature Reviews Neuroscience. 2005; 6:363–375.

Swadlow HA, Gusev AG, Bezdudnaya T. Activation of a cortical column by a thalamocortical impulse. Journal of Neuroscience. 2002; 22:7766–7773. [PubMed: 12196600]

Takeuchi D, Hirabayashi T, Tamura K, Miyashita Y. Reversal of interlaminar signal between sensory and memory processing in monkey temporal cortex. Science. 2011; 331:1443–1447. [PubMed: 21415353]

Tanaka K. Columns for complex visual object features in the inferotemporal cortex: Clustering of cells with similar but slightly different stimulus selectivities. Cerebral Cortex. 2003; 13:90–99. [PubMed: 12466220]

Tomasi D, Volkow ND, Wang R, Carrillo JH, Maloney T, Alia-Klein N, et al. Disrupted functional connectivity with dopaminergic midbrain in cocaine abusers. PLoS One. 2010; 5:e10815. [PubMed: 20520835]

Volkow ND, Wang GJ, Ma Y, Fowler JS, Wong C, Ding YS, et al. Activation of orbital and medial prefrontal cortex by methylphenidate in cocaine-addicted subjects but not in controls: Relevance to addiction. Journal of Neuroscience. 2005; 25:3932–3939. [PubMed: 15829645]

Wagatsuma N, Potjans TC, Diesmann M, Fukai T. Layer-dependent attentional processing by top–down signals in a visual cortical microcircuit model. Frontiers of Computational Neuroscience. 2011; 5:31.

Wang M, Gamo NJ, Yang Y, Jin LE, Wang XJ, Laubach M, et al. Neuronal basis of age-related working memory decline. Nature. 2011; 476:210–213. [PubMed: 21796118]

Weiler N, Wood L, Yu J, Solla SA, Shepherd GM. Top–down laminar organization of the excitatory network in motor cortex. Nature Neuroscience. 2008; 11:360–366.

Zhang M, Alloway KD. Intercolumnar synchronization of neuronal activity in rat barrel cortex during patterned airjet stimulation: A laminar analysis. Experimental Brain Research. 2006; 169:311–325.

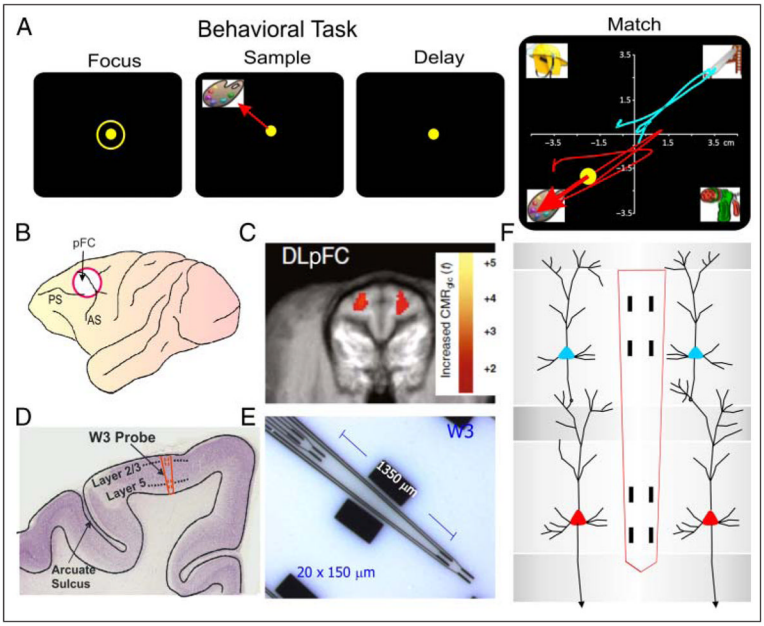

Figure 1.

Interlaminar neuron recording in NHPs performing a visual-motor DMS task, which required movement of a cursor into images projected onto a video screen. (A) Behavioral paradigm showing the sequence of events in the DMS task: (1) presentation of "Focus (Start) Ring" to initiate the trial with cursor placement which produced, (2) presentation of the "Sample Target" image, followed by cursor movement into the image as the "Sample Response" followed by (3) a variable "Delay" period of 1–60 sec with the screen blank which on termination presented the (4) "Match" phase in which the Target (Sample image) was accompanied by 1–6 other nonmatch (distracter) images on the same screen. Cursor movement into the correct (Match target) image for ≥0.5 sec produced a juice reward via a sipper tube mounted next to the animal's mouth. Placement of the cursor into a nonmatch image for ≥ 0.5 sec caused the screen to blank without reward delivery. Intertrial interval: 10.0 sec. (B) Diagram of NHP brain showing pFC recording locations (cortical areas 46, 8, 6). (C) Representative MRI of same dorsolateral pFC (DLpFC) area in B showing PET imaged localized cerebral metabolic rate (LCMRglu) activation (red blots) during DMS task performance (Hampson et al., 2011). (D) Illustrated coronal section in NHP brain showing relative location of supragranular L2/3 and infragranular L5 with tract (in red) used for placement of conformal MEA recording (W3) probes shown in E. (E) Ceramic conformal recording array custom designed (W3) for interlaminar and intercolumnar cortical recording (diagram in F) consisting of dual sets of four recording pads vertically aligned and separated by 1350 μm, the anatomic distance between L2/3 and L5 in primate brain. (F) Dimensionally relevant illustration of the conformal MEA positioned for simultaneous recording from neurons in both layers in adjacent minicolumns (1 and 2), each minicolumn consisting of a "pair" of L2/3 and L5 pFC cells.

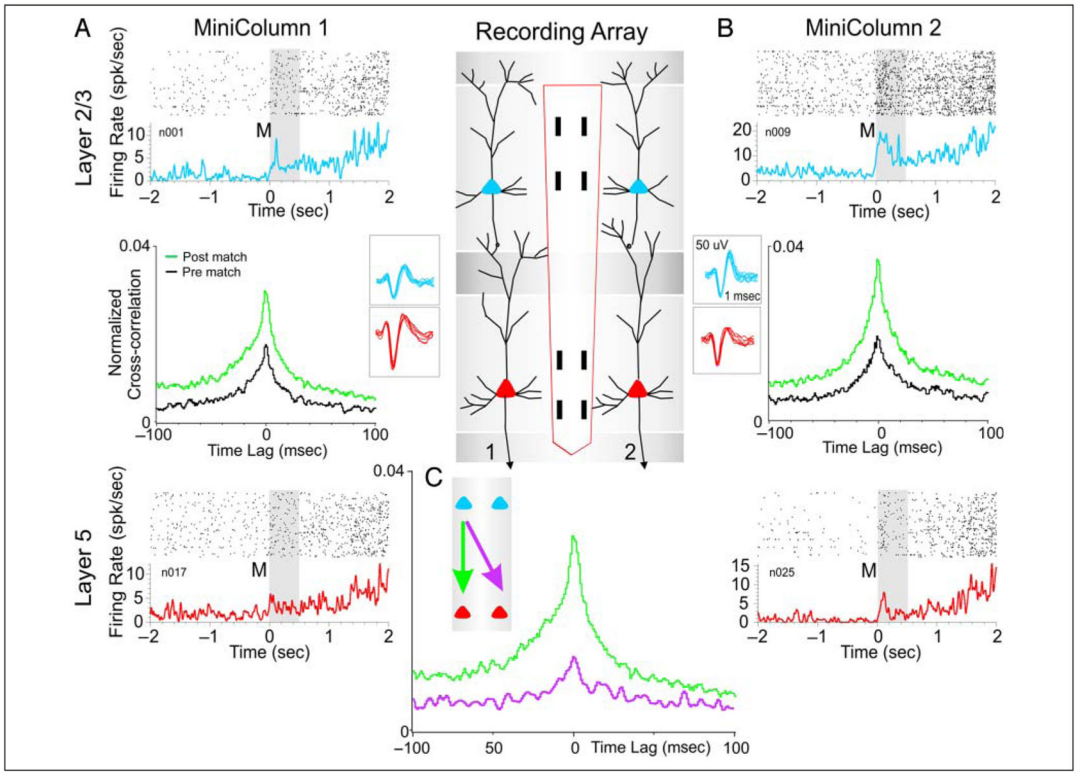

Figure 2.

Interlaminar activity recorded from adjacent prefrontal minicolumns during DMS task performance. Recording array: Center insert shows the conformal MEA positioned for simultaneous interlaminar–columnar recording from adjacent Minicolumns 1 and 2 (Figure 1F) with corresponding L2/3 and L5 cell pair waveforms (blue and red) for results in A and B. (A and B) Individual trial rasters and average perievent histograms (PEHs) obtained from two cell pairs recorded simultaneously from L2/3 (blue) and L5 (red) in minicolumn format over ±2.0 sec relative to Match phase (Figure 1A) onset (0.0 sec) in a single DMS session. CCHs for the same cell pairs in each minicolumn are shown (between raster-PEH displays) in A and B for Pre (black, −2.0 to 0.0 sec) and Post (green, 0.0 + 2.0 sec) time intervals relative to Match phase onset (M, 0.0 sec). CCHs show increased interlaminar synchronization (larger correlation peaks) for both cell pairs during target selection in the Match phase (green, post) relative to similar correlations between the same cell pairs constructed before phase onset (pre, −2.0 to 0.0 sec). (C) Validation of MEA minicolumn selectivity shown by a CCH constructed from a cell pair with same MEA vertical orientation (Minicolumn 1) compared with a CCH constructed from the same L2/3 cell in Minicolumn 1 and the L5 cell recorded on the diagonal, Minicolumn 2, pad of the same MEA (purple CCH) as shown in the inserted diagram.

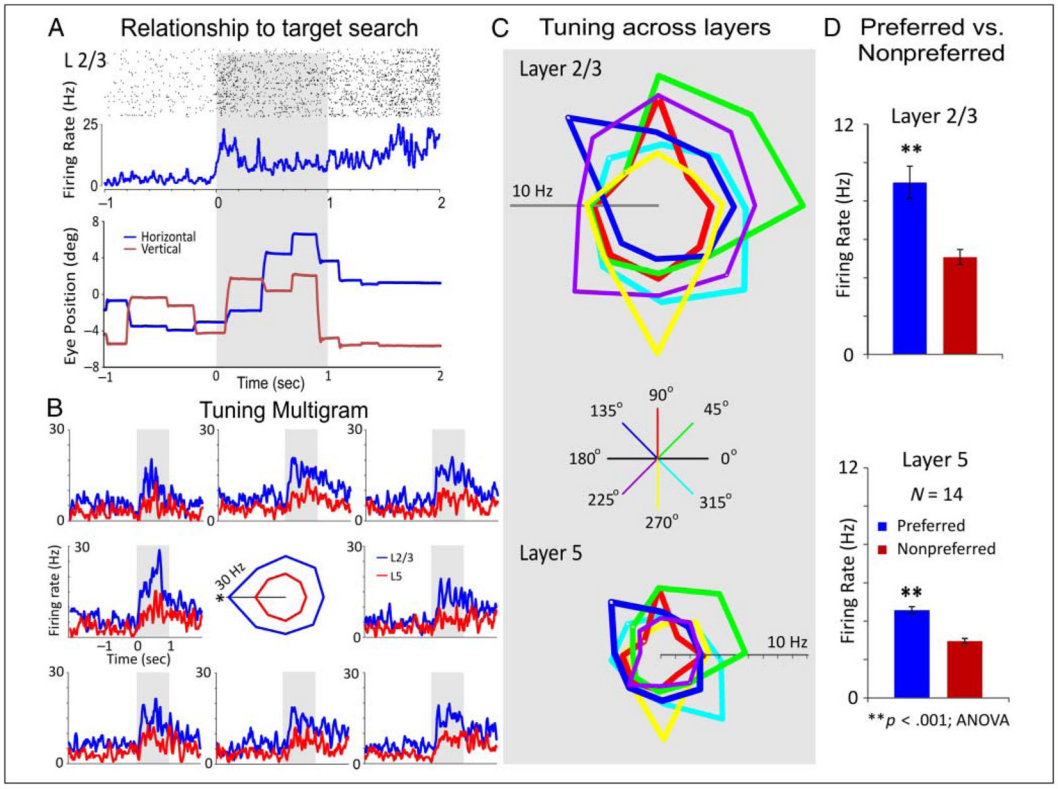

Figure 3.

Minicolumn interlaminar firing associated with target selection movements into different locations on the Match phase screen. (A) Example of functional relationship to match target search. The raster and PEH is for a L2/3 pFC cell that fires during the search for matching target (in gray). Below is shown the time course of eye position (horizontal coordinate in blue and vertical coordinate in red) while making saccadic eye movements during visual search. (B) Tuning plot multigram (Opris et al., 2005b; Rao et al., 1999). Multiple PEHs (multigram) and spatial tuning plot (diagram in center) for two pFC cell pairs, L2/3 (blue) and L5 (red), recorded with the same minicolumnar orientation shown in Figure 2. The spatial tuning plot in the middle displays Match phase mean firing rates (shaded areas in PEHs) along each radial axis corresponding to movement of the cursor into each of the eight screen image positions from the screen center summed over all trials in a single session. The spatial "bias" for minicolumn firing (both cells L2/3 and L5) is indicated by an increased firing rate for target selection in one position (i.e., left; 180° position) versus all others during the session. (C) Comparison of distinct variations in tuning for selected minicolumn cell pairs (L2/3 and L5; $n = 6$). Each of the selected minicolumns show similar tuned Match phase firing for both L2/3 and L5 cells recorded via the MEA, including biases in positions that show the highest rates. Polar coordinates indicate directionality of response movement to one of eight "clock" directions corresponding to the location of the match image (0°, 45°, 90°, 135°, 180°, 225°, 270°, 315°, and 360° relative to center of screen). Amplitude of polar plot corresponds to peak firing rate 0.0–1.0 sec following match presentation. (D) Average firing rate for bias (preferred) and nonbias (nonpreferred) target locations summed across different ($n = 14$) minicolumnar L2/3 and L5 cell pairs.

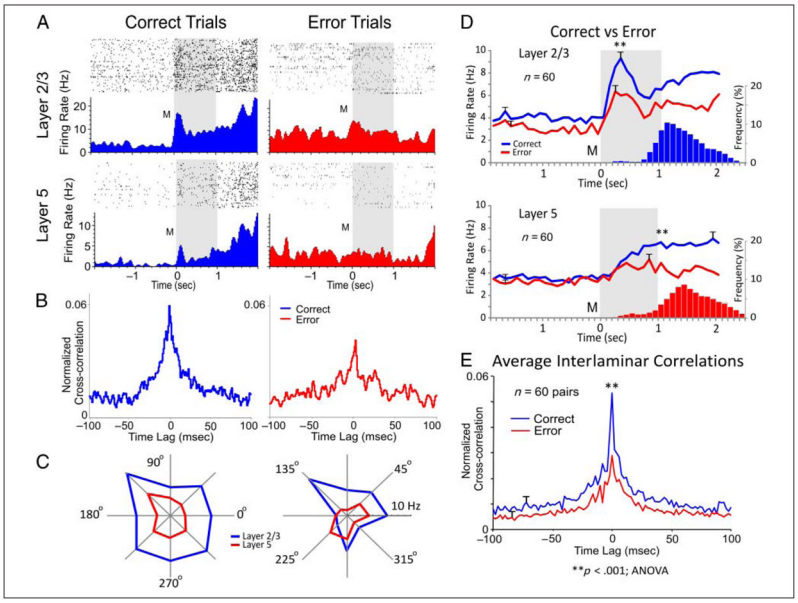

Figure 4.

Differences in pFC columnar processing on correct versus error trials. (A) Match phase individual trial raster-PEHs segregated for correct (blue) and error (red) trials recorded during a 120-trial session from a single, MEA-isolated, interlaminar cell pair as in Figure 2. (B) Normalized cross-correlograms of firing between the same cell pair (CCHs in Figure 2) for correct (blue) versus error (red) trials during the same session shown in A. (C) Tuning plots (Figure 3B) constructed for same cell pair (A and B above) on correct (blue) versus error (red) trials. Tuning bias was 135° for both cells. (D) Mean PEHs during Match phase averaged over all recorded interlaminar pFC cell pairs ($n = 60$), L2/3 (upper) and L5 (lower), on correct (blue) versus error trials (red) summed across animals and sessions with ≥2 cell pairs recorded in same behavioral session from the same MEA. Blue and red histograms (bars) below PEHs show the associated mean frequency distributions of Match Response latencies (in sec) for correct (upper) and error (lower) trials plotted on the same time-base as the PEHs relative to Match phase onset (0.0 sec). (E) Mean CCHs for the same interlaminar cell pairs ($n = 60$) shown in C constructed from correct (blue) and error (red) trials. $F(1, 119) = 14.18$, $^{**}p < .001$ ANOVA, difference in peak mean correlation.

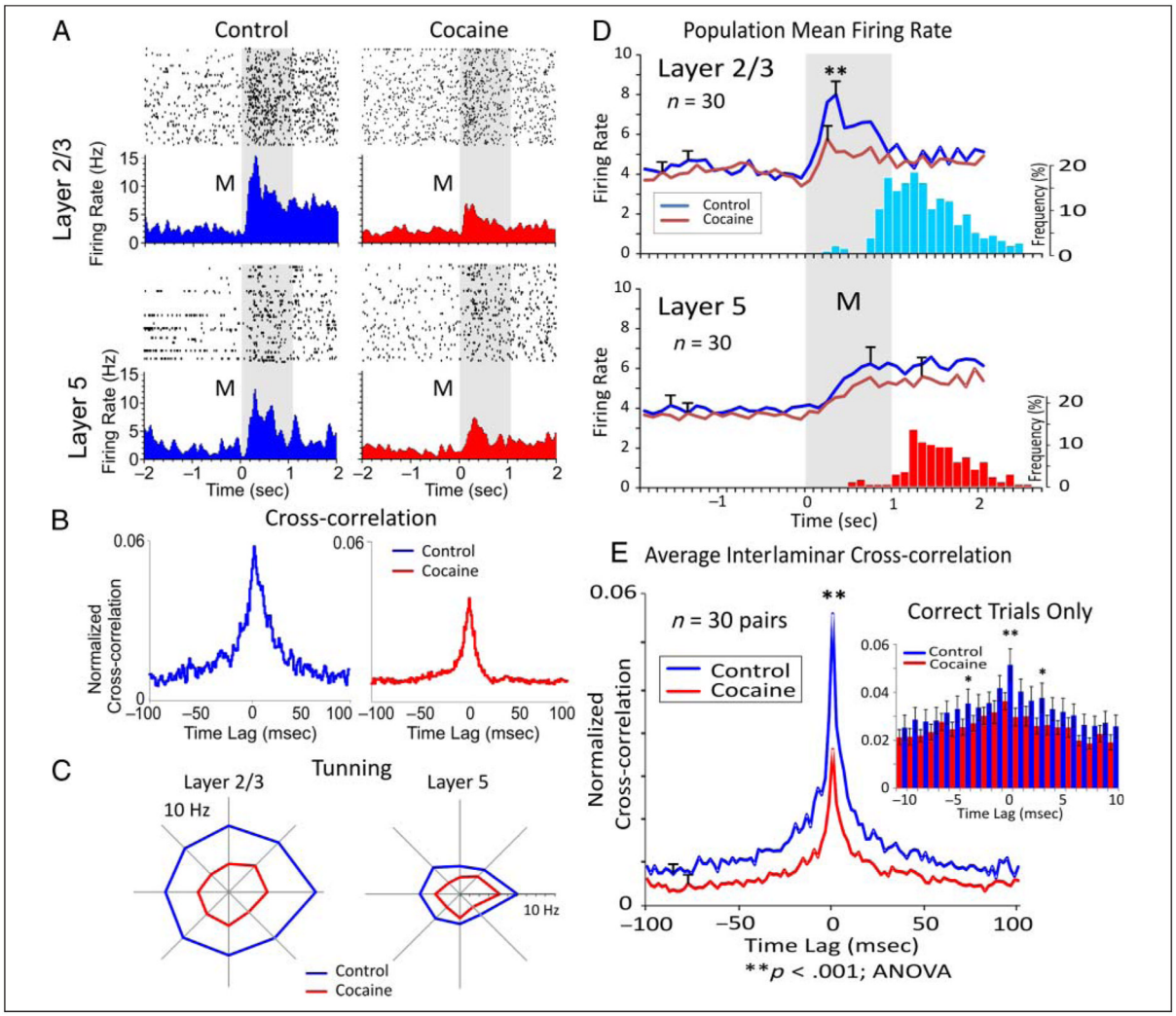

Figure 5.

Cocaine administration (0.40 mg/kg, iv) decreases interlaminar processing necessary for DMS performance. (A) Raster-PEHs show L2/3 and L5 interlaminar cell pair Match phase firing activity as in Figures 1, 3, and 4 during the initial control (saline) half of the session (blue) and after cocaine administration (red) midway through the session. (B) Cross-correlograms of interlaminar cell firing between the same L2/3 and L5 cell pair constructed from all control (blue) trials the first half of the session and trials following cocaine (red) injection during the second half of the same session shown in A. (C) Tuning plots (Figure 3) for the same pair of cells shown in A and B for control (blue) versus cocaine (red) trials during the same session. Tuning bias = 0°. (D) Average PEHs for control (upper) versus cocaine trials (lower) summed over all interlaminar L2/3 (blue) and L5 (red) pFC cell pairs ($n = 30$) recorded in the same sessions in which cocaine was administered midway through. Blue and red histograms show mean frequency distributions of Match Response latencies (Figure 4D) relative to Match phase onset (M, 0.0 sec) for control and cocaine trials respectively. (E) Mean CCHs for same interlaminar cell pairs ($n = 30$) shown in C, constructed from control (blue) versus cocaine (red) trials in the same sessions, $F(1, 59) = 11.22$, $^{**}p < .001$ ANOVA. Inset: Higher resolution CCHs (±10.0 msec) comparing correct trials only (cocaine vs. control half of session) for same L2/3 and L5 cell pairs. Mean (±*SEM*) coefficients, 1.0 msec, $F(1, 298) = 6.65$, $^{**}p < .001$, ANOVA.

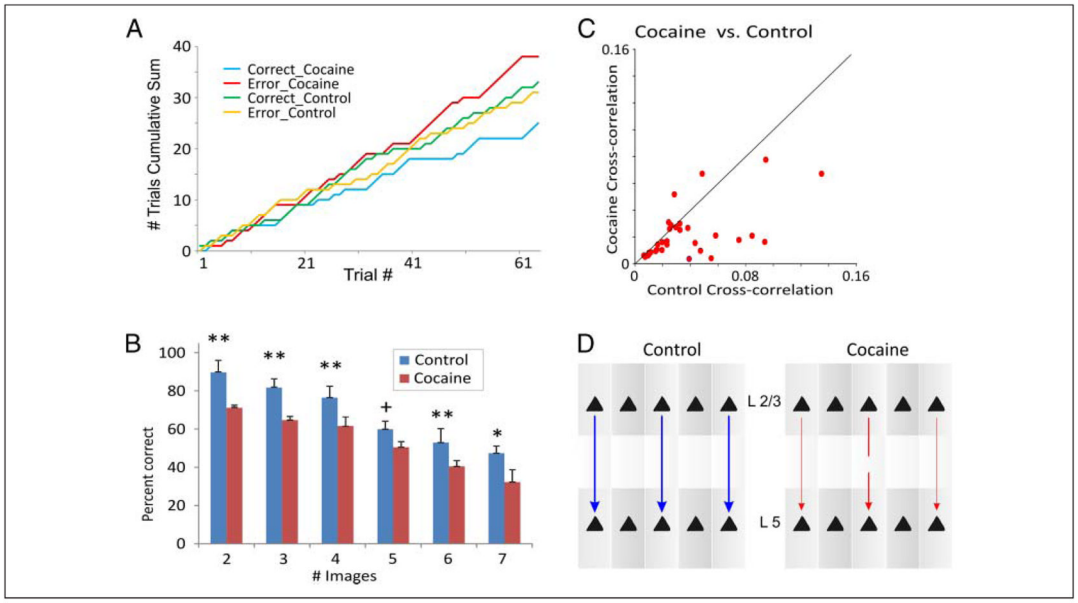

Figure 6.

Cocaine administration alters behavioral and neural correlates of DMS performance. (A) Single session example of the change in cumulative distribution of correct and error trials during the control (saline) versus cocaine halves of the session. Cocaine (0.40 mg/kg) was administered after Trial 62 of the control (saline) half of the session, which reset the cumulative trial plot to 0 (Trial #) for 61 more trials in the cocaine half of the session. Cocaine produced a marked change in the cumulative number of correct (red) and error (blue) trials across the last (61 trials) half of the session compared with the control half of the session where the cumulative trial distribution (green and yellow) was similar. (B) Mean percentage of correct performance across all animals ($n = 4$) for trials with different numbers of distracter images (1–6) in the Match phase during control vs. cocaine halves of the same sessions ($n = 19$). Significance: $^{**}F(1, 96) > 11.22$, $p < .001$; $^{*}F(1, 96) = 10.07$, $p < .01$, $^{+}F(1, 96) = 3.87$, $p < .05$. (C) Scatter plot of normalized cross-correlation coefficients from cell pairs shown in Figure 5C for both the control and cocaine halves of the same DMS session. Lack of distribution along the diagonal line represents a significant change in interlaminar correlated cell firing across the two halves of cocaine administered sessions. (D) Schematic diagram illustrating possible underlying basis for the effects of cocaine administration which produces a partial decoupling of interlaminar correlated firing between cells in pFC L2/3 and L5 as shown in C.